RESEARCH ARTICLE **OPEN ACCESS**

RESEARCH ON CRACK DETECTION OF STEEL PLATE BY PERMEABILITY TESTING TECHNOLOGY

Ling-hui ZHENG, *Shang-kun REN and Yang XU

Key Laboratory of Nondestructive Testing of Education, Nanchang Hangkong University, Nanchang, China 330063

ARTICLE INFO

ABSTRACT

The permeability testing technology is an evaluating method of microstructure changes such as stress concentration and fatigue damage by measuring the change of permeability. In order to explore its ability to detect macroscopic crack defects, a testing platform for permeability was designed, and a physical model of permeability testing crack have been built. Then use the testing platform to detect 45# steel plate which contain artificial cracks from front-side and back-side of it, and the relationship between detection signal and the excitation voltage amplitude was studied. At same time explored the signal characteristics of different detection directions of sensors. The study shows that the sensor has a high signal/noise ratio under the excitation voltage of 5Vpp. The permeability testing method can detect the front-side and back-side crack of the steel plate. When detecting the back-side of the steel plate, the crack at the surface thickness of 2.5 mm can be detected. The research results expand the application field of permeability detection technology and provide a new method for the front-side and back-side detection of steel plate cracks.

INTRODUCTION

Many industrial systems have construction parts, which are fabricated from the most common ferromagnetic construction materials, such as steel or cast iron (Wu, 2009). Steel components are bored different forms of destructive factors loads for a long time, then the microstructure of specimens may change or even crack. So efficient and reliable nondestructive testing (NDT) technology is vital for the early diagnosis of engineering equipment (Rabung, 2014). Scholars at home and abroad have done a lot of research and made some achievements in detecting the micro variation of the internal structure of ferromagnetic materials by using permeability. The initial permeability is expressed as the initial stage of the magnetizing process property, which is the ratio of the magnetic induction intensity to the magnetic field strength, and material. The initial permeability μ of ferromagnetic material varies with the intensity of magnetic field H. According to the initial permeability change under low field condition, the sensitivity of measuring stress concentration and fatigue

Corresponding author: Shang-kun REN,
Key Laboratory of Nondestructive Testing of Education, Nanchang Hangkong University, Nanchang, China 330063

damage condition will be more sensitive (Ren, 2009 and Ren, 2014). By extracting and detecting the voltage signals in the induction coil, the initial permeability of ferromagnetic material can be reflected (Tomáš, 2004). Detection technology based on the initial permeability is a new non-destructive evaluation method, the micro-structure damage changes of ferromagnetic specimen can be detected by the and change of initial permeability, stress concentration, fatigue damage and micro-structural changes of the component can be evaluated in early (Tomáš, 2006; Ren, 2010 and Ren, 2009). Various magnetic properties measured from major loops and minor loops have been found to be sensitive to different microstructural features and have shown different behaviours in response to microstructural changes for power generation steel P9 and T22 in the different conditions (Liu, 2012). Magnetic Adaptive Testing (MAT) technology could detected relatively small, local modification of the sample thickness from the other side of the specimen with good signal/noise ratio. Also good results if the investigated plate was covered by other plates (Vétesy, 2012). The magnetic permeability is approached by Taylor series progression, and the relationship between magnetic induction field, magnetic field and cable tension stress is deduced (Ktena, 2014).

On the basis of previous researches, the crack of ferromagnetic plate was experimentally studied by using the permeability characteristics (Wu, 2017). Only by scanning the surface permeability of ferromagnetic materials, the defect information of ferromagnetic materials can be obtained. The test expands the application field of magnetic permeability detection technology and provides a new method for front-side and back-side crack detection of steel plate.

Relationship model between the detection signal and permeability

In this paper, a probe is designed for evaluating the quality of steel plate with magnetic conductivity detection method. The yoke is an "M" shaped Mn-Zn ferrite. An excitation coil is wound on the middle leg and a detection coil is wound on the left and right legs of the yoke. The left and middle leg of the yoke and the specimen to be tested constitute a closed magnetic circuit called "Detection Circuit", while the right leg and middle leg of the yoke and the specimen to be tested form another closed magnetic circuit called "Reference Circuit". The detection signal is output as a differential voltage. The structure of probe is shown in Figure 1.
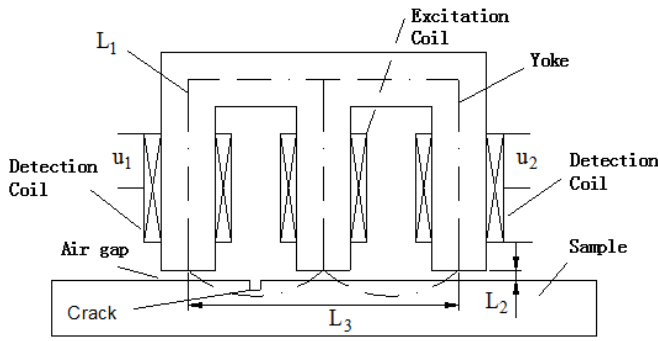

Fig. 1. Sensor structure diagram

For each closed magnetic loop, based on Abe's loop theorem and Ohm's of magnetic circuit:

$$\phi = \frac{N_1 i}{\dfrac{L_1}{\mu_1 S} + \dfrac{2L_2}{\mu_2 S} + \dfrac{L_3}{\mu_3 S}} \tag{1}$$

In equation(1), ϕ express the magnetic flux, μ_1 express permeability of probe core, μ_2 express permeability of air, μ_3 express permeability of specimen, L_1 is the length of probe, L_2 is the length of air, L_3 is the length of specimen, N_1 express the number of turns of the excitation coil, i express excitation current of the yoke, S express the average equivalent cross-sectional area. According to Maxwell second equation:

$$\oint_L E \cdot \mathrm{dl} = -\int_S \frac{\partial B}{\partial t} \cdot ds , \quad \text{flux density: } B = \phi / S \text{ ,the output}$$

signal can be obtained:

$$u_{out} = \frac{N_1 N_2}{\dfrac{L_1}{\mu_1 S} + \dfrac{2L_2}{\mu_2 S} + \dfrac{L_3}{\mu_3 S}} \frac{d_i}{d_t} \tag{2}$$

N_2 express the number of turns of the detecting coil. Formula (2) indicates that when the permeability μ_3 of the specimen to be changed, the output signal can change correspondingly. Due to macroscopic defects, such as cracks in components can affect the permeability, so could infer the size and location of defects inside or on the surface of specimen by the change of output signal voltage amplitude. Fig.1 shows that the probe takes the difference between the signal u_1 of the "Detection circuit" and the signal u_2 of the "Reference Circuit" as the output signal Δu. According to the principle of differential cancellation, when there are no macroscopic defects such as cracks in the magnetic loop area at the "Detection Circuit" or the "Reference Circuit" of the probe, the signal difference between them is zero. However, when any of the two circuits have defects, the signal difference between the two circuits changes significantly, so as to realize the detection of macroscopic defects such as cracks. In the actual application process of the probe, it was found that the signal difference between the two circuits of the probe is not zero even in the defect free area of the steel plate. The detection magnetic circuit cannot be exactly the same as the reference magnetic circuit, so the output will only be a value approaching zero.

Put the ac signal Δu output by the probe through the amplification and rectification of signal conditioning circuit, and the final voltage output is:

$$X = \frac{L_1}{\mu_1 S} + \frac{2L_2}{\mu_2 S} + \frac{L_3}{\mu_3 S} \quad Y = N_1 N_2 \frac{d_i}{d_t}, \tag{3}$$

$$U = A \cdot \frac{\sqrt{2}}{2} \cdot \left| \Delta u \right|_{\max} \tag{4}$$

$$U = \frac{\sqrt{2}}{2} A N_1 N_2 \omega i_{\max} \cdot \frac{Y L_3 \Delta \mu_3}{S \mu_3^2 X^2 - (S \mu_3 X^2 - X L_3) \Delta \mu_3} \tag{5}$$

It can be seen from the formula (5) that the change of μ_3 is related to the detection signal. The value of variable X can be controlled to obtain higher detection accuracy. On the premise of satisfying the optimal detection accuracy, the magnetic core length of the detection probe and the cross-sectional area of the wound magnetic core should be reduced appropriately, and the magnetic core material with high initial permeability should be used to make the magnetic core of the probe, and the lift-off effect should be avoided to increase the detection sensitivity. The detection conditions of magnetic circuits on both sides of the probe are the same, and the common-mode interference between them can cancel each other. In equation (4), the output signal/noise ratio of no interference signals is greatly increased, and macroscopic defect signals such as cracks are highlighted.

Test equipment and test methods

Test platform device includes the following sections: excitation signal source, excitation coil, detection coil, oscilloscope, "M" magnetic yoke, steel plate to be tested, low-pass filtering and signal conditioning circuit. "M"-shaped yoke chooses high permeability Mn-Zn ferrite material, whose permeability is $3500\mu_0$ ($\mu_0 = 4\pi \times 10^{-7} H/M$). Select 45 steel plate

with a permeability of $600\mu_0$ as the test object, the overall dimensions of 400mm×120mm×12mm shown in Fig. 2.
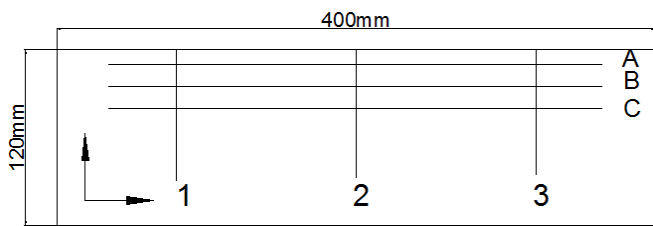

Fig. 2. Steel plate diagram

There are three crack slot in the steel plate with an interval of 87mm, the length of crack is 80mm, the width is 3mm, the depth of crack is 11mm, 10mm, 9.5mm respectively numbers 1, 2 and 3. Corresponding to the surface layer thickness on the back-side crack, the Numbers 1', 2'and 3' are respectively 1mm, 2mm and 2.5mm. In addition, all three crack grooves cut an arc surface at 55mm, the cross-section of no.1'crack groove is shown in Fig 3. In the test, take the point 0 on the left side of the crack-free steel plate and scan it to the right along the route A, B and C successively, passing through at position *L* mm of the steel plate. The direction of probe moves on the surface of the steel plate was divided into two kinds. One is move on the sample surface along a direction parallel to the axis of the crack, which is called lateral scanning. The other is along a direction perpendicular to the axis of the crack, which is called longitudinal scanning. The excitation coil was wound on the middle leg of "M" magnetic yoke, with N_1=100 turns and the detection coil was wound on left and right leg of the yoke with N_2=100 turns. The coil is made of copper enameled wire with a sectional area of $0.0573mm^2$. Excitation coil is fed by sinusoidal alternating current V=2Vpp, f=120Hz.

The relationship between different detection surfaces and detection signals: The detection results of probe along the three paths of A, B and C show the same trend. Therefore, the detection signal on path B is only analyzed (The detection signal is the differential voltage output of the sensor between the detection end of the "M" probe and the defect position of the specimen to be tested). The mean value of the signal detected by the probe in the absence of defects is defined as noise signal. Under 2Vpp excitation voltage, the sensor longitudinally scans the front-side and back-side of the steel plate, and the test results are shown in Fig.4. We can see in Fig.4(a), the detection signal of different crack on the front-side of the steel plate changes significantly compared with the noise signal, calculated number 1.2.3 crack relative noise signal variation respectively ΔV_1=1.96Vpp, ΔV_2=2.18Vpp, ΔV_3=1.9Vpp, Fig.4(b) for the back-side plate crack detection signal, by calculating the number 1. 2. 3 crack groove relative noise signal variation respectively $\Delta V_1'$=1.32Vpp, $\Delta V_2'$=0.88Vpp, $\Delta V_3'$= 0.33Vpp. While the steel plate has no defects, the noise signal fluctuates, which is caused by the uneven surface, local stress concentration and lift-off effect caused by mechanical wear during the processing of the steel plate. The defect on the front-side of the steel plate shows a signal diagram of a shape similar to "M". The reason is that the probe was scanned on the steel plate, its detection circuit and reference circuit will pass through the same defect successively. Therefore, two signal peaks of similar shape and size appear in the detection result curve, which is called "M" shape defect signal diagram.
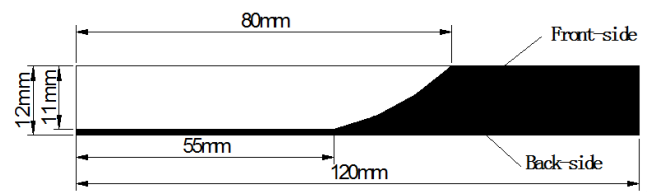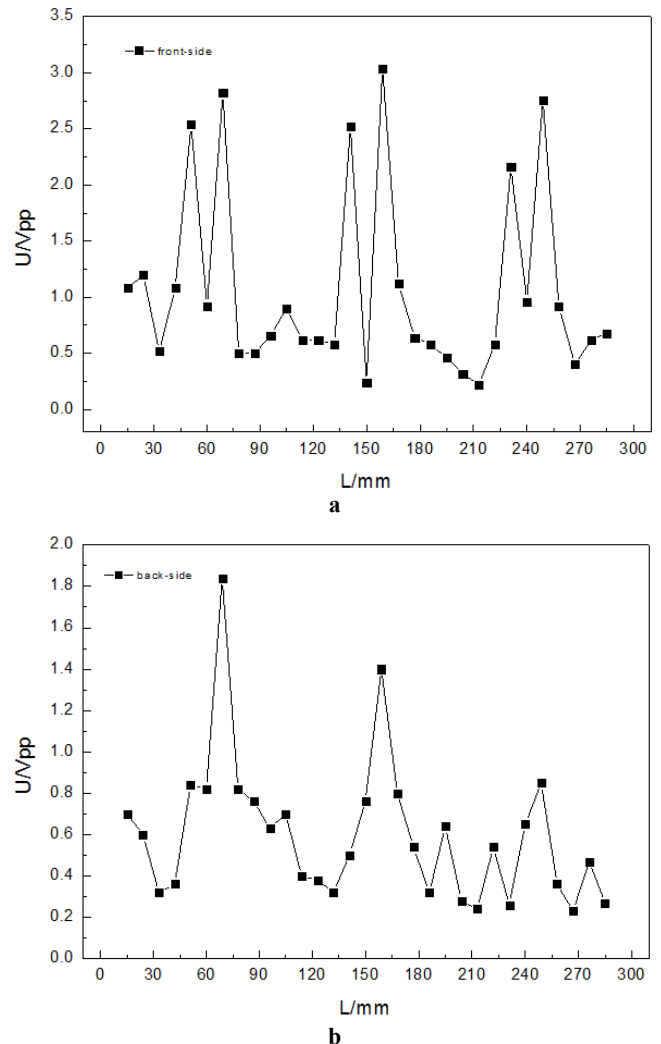

Fig. 3. Diagram of cross-section of crack no.1

a

b

Fig. 4. Longitudinal scanning results of front (a) and back (b) of steel plate under 2Vpp excitation voltage

The relationship between different excitation voltages and detection sensitivity: When the probe longitudinal scanning on the surface of the back-side of sample to detect defect, the detection signals first increases and then decreases, presenting a single peak pattern, as shown in Fig. 4(b), which is significantly different from the "M" shape defect signal appearing in the front-side detection results. The amplitude of the back-side detection signal decreased significantly compared with the front-side. Under the excitation of 2Vpp, the sensor has a good ability to identify cracks at surface depths of 1mm and 2mm. However, when the surface depth reaches 2.5mm, the defect signal is buried in the noise signal, and different surface depths correspond to different signal amplitudes. In order to verify whether the detection method has the ability to detect the back-side defect crack of 2.5mm, the excitation voltage is increased and the magnetic flux of the magnetic circuit is increased. The results are shown in Fig.5 Fig.5 shows the distribution rules of detection signals under different excitation voltages Fig.5 express excitation voltage is 3-6Vpp, with the increase of the excitation voltage, the

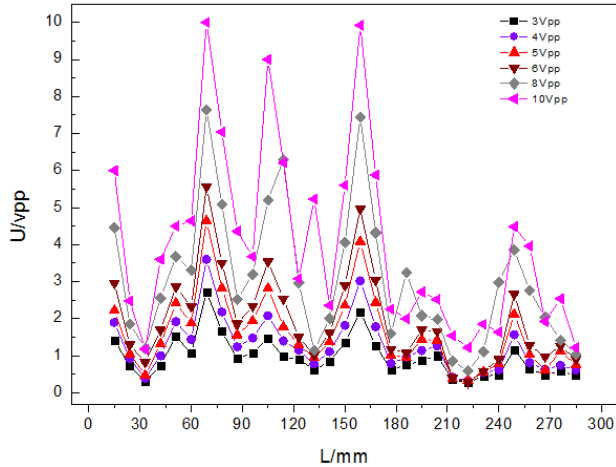detection signal is gradually increasing, and the sensor has a good suppression of noise signal.

Fig. 5. Detection signal distribution law under different excitation voltage

When the excitation voltage is greater than 6Vpp, the sensor vibrates slightly and generates minimal attraction. This has caused interference to the detection, and the defect cannot be determined, so the upper limit of excitation voltage is 6Vpp. In order to reduce the influence of non-uniformity in the absence of defects on the signal, let $U_A = \sum_A^m u_i / N$, $\delta u = U_i - U_A / U_A$.

U_A express the signal mean at the defect free place; δu express the relative increase of the signal mean at the defect free place; U_i express the detection signal. The larger δu is, the higher the signal/noise ratio will be.
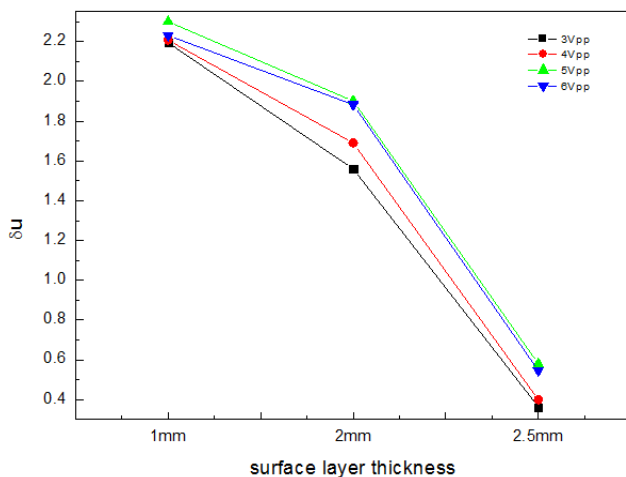

Fig. 6. The variation of u with surface layer thickness under different excitation conditions

Fig.6 shows the relationship between δu value and surface layer thickness under different excitation conditions. It can be seen that 5Vpp is the best excitation voltage of the sensor, with the highest signal/noise ratio.

The relationship between different ports of the probe and detection signal: After study of the "M"-shape signal in figure 4, it is not difficult to see that the signal at the detection end and the reference end of the probe are different from each other when encountering defects. There is a signal rule that the first wave peak of the "M"-shape is smaller than the second wave peak. The test was carried out by using an arc face at the 1'end of a prefabricated crack groove. The probe starts from the defect free position. Three representative lateral scanning paths were specially selected :(1) the crack was at the center of

the detection end; (2) the crack was at the bottom of the intermediate excitation yoke; (3) the crack was at the center of the reference end. By scanning the front-side and back-side respectively, the resulting curves are shown in Fig.7.
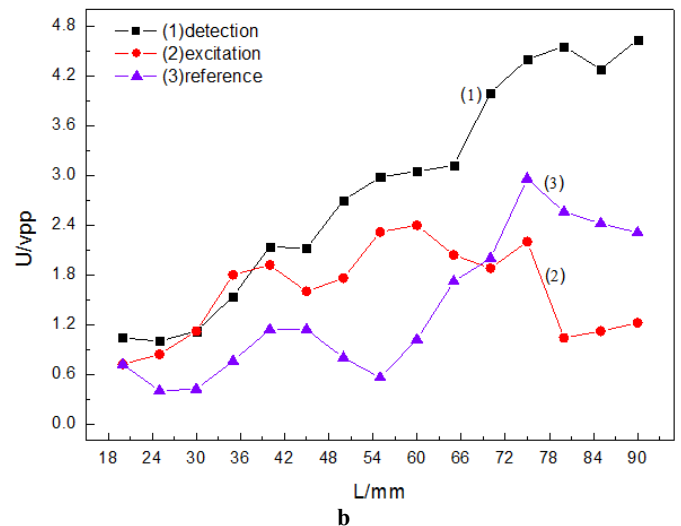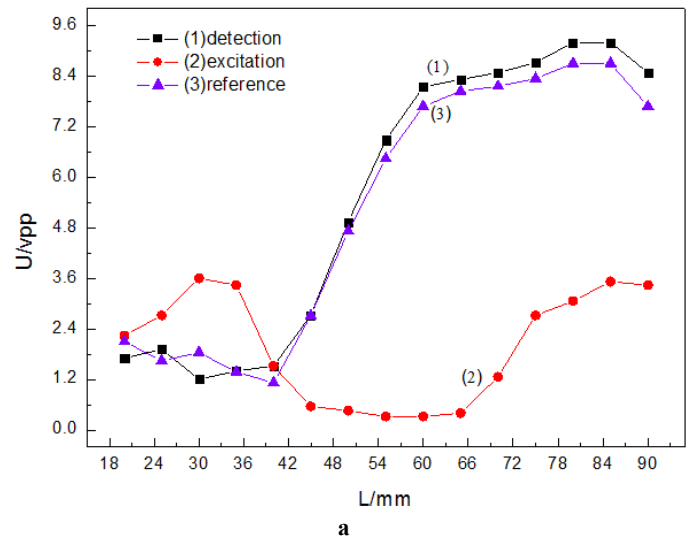

a

b

Fig. 7. Lateral scan results for the front-side (a) and back-side (b) of the probe with different ports

Fig.7 shows that at the beginning of the detection without defects, the signal change is small because there is no potential difference between the two ends. For the front-side of the steel plate, after the sensor encounters defects, the voltage of the detection end is slightly higher than that of the reference end, which is consistent with the asymmetry of "M" signal in Fig.4(a). Both ends have high sensitivity to defects, but the relative change of signal at the detection end ΔV=6.78Vpp, is greater than that at the reference end ΔV=5.58Vpp,When crack is encountered at the intermediate excitation yoke, the detection signal changes little. Fig.4(b) show that the sensor on the back-side detects the corresponding position, the detection signal is small compared with the front detection signal, the background signal is little different from the reference signal, and the detection end signal is large, so the "M" shape of the detection signal is not obvious. This is why there is no "M" signal when scanning for defects on the back.

Conclusion

The above described experiments showed that permeability testing technology was an effective tool for nondestructive

detection on Crack of steel plate. The method gave good results for cracks under the back-side surface of steel. According to the test detection model provided above, the crack could be well detected under the surface thickness of 2.5mm. At the excitation voltage of 5Vpp, the probe had a good signal/noise ratio. There is a good distinction between the detection signal with M-shaped feature in the front crack groove and the single-peak signal of the back crack, and the change of the detection signal of the front-side crack is much greater than that of the back-side crack. It is expected that good results can be achieved on the case of deeper surface thickness of the steel plate. Systematic experiments on more sophisticated samples will be performed in the near future, with the intention to determine minimal detectable size of crack in given plates, and generally to optimize the structure and precision of the probe in the whole measurement.

Acknowledgement

REFERENCES

Ktena A, Davino D, Visone C, *et al*. stress dependent vector magnetic properties in electrical steel *[J]. Physica B: Condensed Matter,* 2014, 435:25-27.

Liu J, Wilson J, Strangwood M, *et al*. Magnetic characterisation of microstructural feature distribution in P9 and T22 steels by major and minor BH loop measurements [J]. *Journal of Magnetism and Magnetic Materials,* 2016, 401(3):579- 592

Rabung M, Altpeter I, Boller C, *et al*. Non-destructive evaluation of the micro residual stresses of IIIrd order by using micro magnetic methods[J]. *NDT & E International*, 2014, 63(4):7-10.

Ren S K, Fu R Z, Li X L, *et al*. Influences of environmental magnetic field on stress-magnetism effect for 20 steel ferromagnetic specimen[J]. Insight: *Non-Destructive Testing and Condition Monitoring,* 2009, 51(12):672-675.

Ren S K, Ou Y C, Fu R Z, Fu Y W. Studies on stress-magnetism coupling effect for 35 steel components [J]. Insight: Non-Destructive Testing and Condition Monitoring, 2010, 52(6):305-309.

Ren S K, Song K, Li X L. Influences of environmental magnetic field on stress-magnetism effect for 20 steel ferromagnetic specimen [J]. Insight: Non-Destructive Testing and Condition Monitoring, 2009, 51(12):672-675.

Ren S K, Xu Z H. Sensitive differential permeability evaluation technique for strain damage and microstructure transformation of ferromagnetic specimens[J]. *Journal of Aeronautics,* 2014, 35(5):1452-1458.

Tomáš I, Stupakov O, Kadlecová J. Magnetic adaptive testing-low magnetization, high sensitivity assessment of material modifications [J]. *Journal of Magnetism and Magnetic Materials,* 2006, 304(2): 168-171.

Tomáš I. Magnetic Adaptive Testing Magnetic of Non-magnetic Properties of Ferromagnetic Materials [J]. *Journal of Physics,* 2004, 54(4):23-26.

Tomáš I. Non-destructive magnetic adaptive testing of ferromagnetic materials [J]. *Journal of Magnetism & Magnetic Materials,* 2004, 268(1):178-185.

Vétesy G, Tomáš I, Uchimoto T, Takagi T. Nondestructive investigation of wall Thining in layered ferromagnetic material by Magnetic Adaptive Testing [J]. *NDT & E International,* 2012, 41(4): 51-55.

Wu C J, Chen G L, Qiang W J. Metal materials science 2009. Beijing Metallurgical Industry Press

Wu, D H, Liu Z T, Wang X H. A new method for nondestructive testing of ferromagnetic materials based on differential magnetic permeability [J]. *Journal of Scientific Instrument,* 2017, 38(6): 1491-1497.

****